Environ. Sci. Technol. **1999**, *33,* 1627−1636

Quantitative Speciation of Lead in Selected Mine Tailings from Leadville, CO

JOHN D. OSTERGREN,*,† GORDON E. BROWN, JR.,†,‡ GEORGE A. PARKS,† AND TRACY N. TINGLE§

Department of Geological & Environmental Sciences, Stanford University, Stanford, California 94305-2115, Stanford Synchrotron Radiation Laboratory, SLAC, Stanford, California 94309, and Center for Materials Research, Stanford University, Stanford, California 94305

We have characterized Pb speciation in selected tailings from the Leadville, CO, area using a variety of analytical techniques, including X-ray absorption fine structure (XAFS) spectroscopy. Samples from three locations were analyzed, including two chemically distinct tailings piles located within the city limits [Apache (pyrite-rich, low pH) and Hamms (carbonate-rich, near-neutral pH)] and tailings material deposited as overbank sediments along the Arkansas River approximately 13 km downstream from Leadville (Arkansas River tailings). Extended XAFS (EXAFS) spectra of these multicomponent samples were fit using linear combinations of model compound spectra. In accordance with pH differences among the samples, adsorbed Pb accounts for ~50% of total Pb (Pb_T) in fine fractions of the near-neutral pH Hamms tailings, whereas Pb-bearing jarosites account for the majority of Pb_T in the fine fractions of the low pH Apache and Arkansas River tailings. EXAFS analyses following sequential extraction by $MgCl_2$ and EDTA show evidence of significant redistribution (readsorption) of Pb during the $MgCl_2$ extraction and for removal of adsorbed Pb and dissolution of Pb-carbonates during the EDTA extraction. Changes in Pb speciation with water extraction (dissolution of anglesite and precipitation of plumbojarosite) are observed in one sample of Arkansas River tailings. These molecular-scale results show that Pb speciation varies dramatically among environments in the Leadville area and that Pb occurs in a number of phases not amenable to definitive characterization by conventional microanalytical and/or chemical extraction techniques.

Introduction

More than 130 years of mining and smelting in Leadville generated large quantities of waste materials, including waste rock, tailings, and slags. The potential health risks and environmental hazards posed by these wastes prompted the U.S. Environmental Protection Agency (EPA) to place the area on its National Priority (i.e., Superfund) List 1983. Since that time, a number of investigations have assessed the relationships among metal speciation, mobility, and bioavailablility in the Leadville area (e.g., refs *1*−*4*) (the term speciation as used here includes oxidation state, molecular structure, and phase association, including the mode of surface attachment for adsorbates and both the structure and composition of precipitate phases). For example, in vivo swine studies have shown that Pb bioavailability ranges from less than 5% for tailings materials where the majority of total Pb (Pb_T) occurs as galena (PbS) to 45% for surface soils where the majority of Pb_T occurs as "Fe−Mn−Pb oxide" phase(s) (*4*). Distinguishing between and characterizing such species therefore provides the foundation for identifying and understanding the geochemical processes that control metal transport and bioavailability in environmental media.

While great progress has been made in recent years applying modern microanalytical techniques, such as scanning electron microscopy (SEM) and electron probe microanalysis (EPMA), to determine Pb speciation in environmental samples (e.g., refs *5* and *6*), these techniques are not well suited to characterizing a number of species that may pose significant threats to human health and the environment. For example, their insensitivity to submicron scale chemical and/or physical heterogeneities precludes definitive characterization of materials such as fine-grained and/or poorly crystalline (hydr)oxides of Fe and Mn which play important roles in metal bioavailability and transport in the Leadville area (e.g., refs *1* and *3*) and elsewhere (e.g., refs *7*−*9*). Distinguishing between, for instance, adsorption to and (co)precipitation with such materials is basic information needed to understand and predict metal fate in natural systems. Surface-specific spectroscopies (e.g., XPS, SALI, and SIMS) have been used to identify sorbed metals in environmental materials (e.g., refs *10* and *11*), but the chemical speciation information derived from these techniques on environmental samples has thus far been limited.

In this study, we characterize Pb speciation in selected tailings materials from the Leadville area using a variety of analytical methods, including X-ray absorption fine structure (XAFS) spectroscopy. On the basis of previous work in the Leadville area (e.g., refs *12*−*15*), three different tailings deposits were selected for analysis in the present study, including two chemically distinct tailings piles located within the city limits (Apache and Hamms) and tailings material deposited as overbank sediments along the Arkansas River approximately 13 km downstream from Leadville (Arkansas River tailings) (see Supporting Information for site map). The Apache and Hamms tailings represent endmembers in tailings composition in the Leadville area, the Hamms being carbonate-rich with a near-neutral pH (*6*−*8*), and the Apache being sulfide-rich with a correspondingly low pH (2−6) (*13*). This difference in pH is expected to have a dramatic affect on the type(s) of sorbed species found in these materials. Our primary goal in analyzing Pb speciation in the Arkansas River tailings materials was to provide a more detailed understanding of why the lability of Pb changes so dramatically between samples collected along a vertical cross-section as reported earlier for these samples (*15*).

As a probe of local structure, XAFS spectroscopy is well suited to characterize and distinguish among the many fine grained and/or poorly crystalline Pb species found in tailings materials. In lieu of direct analytical techniques, these materials are commonly characterized indirectly by chemical extraction techniques (e.g., refs *1*, *3*, and *7*−*9*). Although problems such as nonselectivity and redistribution of phases during extraction are well documented (e.g., refs *16*−*18*),

* To whom correspondence should be addressed at Stanford University, Building 320, Room 118. Phone: (650) 723-7513. Fax: (650) 725-2199. E-mail: johno@pangea.stanford.edu.
† Department of Geological & Environmental Sciences.
‡ Stanford Synchrotron Radiation Laboratory.
§ Center for Materials Research; deceased.

10.1021/es980660s CCC: $18.00
Published on Web 04/03/1999

these extractions are designed and commonly interpreted to *selectively* extract specific species and/or classes of species (e.g., refs *1*, *8*, *9*, *19*, and *20*). In this study, we also evaluate the effects of two such chemical extractions ($MgCl_2$ and EDTA) by analyzing materials before and after extraction by XAFS spectroscopy. XAFS methods are reviewed in a number of previous publications (e.g., refs *21*−*23*), and their application to determining metal(loid) speciation in natural materials has also been discussed in several recent papers (e.g., refs *24*−*29*).

Experimental Section

Sample Collection. Composite grab samples were collected from the upper 10 cm of the Hamms and Apache tailings piles in June, 1995. Samples from Arkansas River tailings overbank deposit were collected from a single continuous core at 5 and 13 cm below ground surface in 1996 and received from the U.S. Geological Survey (USGS) in November, 1997; related analyses of these samples were published previously [core 10 as presented by Smith et al. (*15*)]. Since the time of our sampling, the Hamms tailings pile has been composited with other mine wastes and capped under the auspices of the ongoing EPA remediation project.

Bulk Chemistry and Mineralogy. Tailings samples were analyzed by standard commercial methods for bulk chemistry (ICP with aqua regia digest and/or XRF), and by powder X-ray diffraction (XRD) for crystalline phase identification. Consistent with previous investigations of these materials (*13*, *14*), our sample of the Apache tailings is rich in sulfides (especially pyrite) and has a correspondingly low pH, while our sample of the Hamms tailings contains abundant carbonate and has a near-neutral pH (Table 1). As presented in a previous study, the two Arkansas River tailings samples have comparable total Pb concentrations (5 cm, 2500 ppm; 13 cm, 3500 ppm) but dramatically different water extractable Pb concentrations [5 cm , 3450 μg/L; 13 cm, 300 μg/L (3 h in 2 g of sample/40 g of DDI water suspensions)], and XRD analyses indicate that the 5 cm sample contains approximately 70% pyrite and 7% jarosite, whereas the 13 cm sample contains only 5% pyrite but has somewhat more jarosite (17%) (*15*).

Size Separation. Fine fractions of the Apache and Hamms tailings as well as the water-extracted Arkansas River tailings were isolated by sedimentation from suspension in deionized water. Supernatants containing suspended fines were decanted and centrifuged after settling times defined to achieve a desired maximum particle size. Settling times were less than 15 min in all cases, although total exposure to bulk water prior to size separation was approximately 6 months for the "water-extracted" Arkansas River tailings samples. Following centrifugation, samples of the supernatant (0.2 μm filtrate) were collected for analysis; Pb concentrations in these supernatants were below detection (<350 μg/L) in all cases except for the "water-extracted" 5 cm sample of the Arkansas River tailings, which contained 2250 μg/L. Fine fractions (<250 μm) of the nonextracted Arkansas River tailings materials were isolated by dry sieving through nylon screens. Fine fractions for XAFS analyses were loaded into Teflon sample holders immediately following size separation, and samples for other analyses (XRD and EPMA) were allowed to dry at room temperature and pressure. Samples subjected to chemical extraction were size fractionated by sedimentation in the final rinse solution (see below).

Chemical Extractions. Materials from the Hamms and Apache tailings were subjected to a two-step sequential extraction procedure consisting of $MgCl_2$ followed by EDTA. The $MgCl_2$ extraction followed the method described by Tessier et al. (*30*), and the EDTA extraction followed a procedure used previously on materials from Leadville (*13*).

TABLE 1. Bulk Chemistry and Mineralogy[a]

	Apache tailings	Hamms tailings	alluvial tailings (5 cm)	alluvial tailings (13 cm)
pH	2.7	6.8		
major elements (wt %)				
Na	0.03	0.03	0.03	0.04
Mg	0.31	2.43	<0.01	0.02
Al	0.54	0.56	0.02	0.14
P	0.12	0.16	<0.01	0.02
K	0.32	0.18	0.07	0.19
Ca	3.99	4.00	0.13	0.48
Fe	16.4	6.18	34.0	4.87
trace elements[b] (ppm)				
V	10	10	34	9
Cr	7	11	11	4
Mn	1210	8320	136	74
Cu	1170	502	118	63.2
Zn	7970	>10 000	7660	2440
As	393	175	479	122
Ag	49.0	30.9	>100	38.2
Cd	31	97	67	16
Pb	8330	8520	15 660	8250
organic carbon (wt %)	0.27	<0.01	na	na
bulk mineralogy[c]				
quartz	25	30	y	y
pyrite	25	x	70	5
Ca (±Mg, Fe) carbonates	x	35		
Fe-rich (hydr)oxides	x	15		
sphalerite	x	x		
clay (illitic)	x	x		
gypsum	x			
jarosite	x		7	17

[a] Bulk chemical data are for <100 μm size fractions of the Hamms and Apache tailings and <250 μm size fraction of the fluvial tailings sample. [b] "Trace" elements as distinguished by convention, in spite of relatively high concentrations in some cases (i.e., Zn, Pb, and Mn). [c] Bulk mineralogy as determined by XRD and EPMA. Volume percentages based on EPMA. "x" detected, but less than 10% by volume; "y" detected by XRD, but not quantified.

High ionic strength neutral salt solutions, such as the 1 M $MgCl_2$ extraction used here, are intended to remove electrostatically bound outer-sphere surface complexes by flooding the system with alternate ions, whereas EDTA has been used to selectively dissolve poorly crystalline Fe (hydr)-oxides (and associated metals) (e.g., ref *31*), carbonate minerals (e.g., ref *32*), and chemically bound inner-sphere surface complexes (e.g., ref *19*).

The $MgCl_2$ extraction consisted of suspending the solids for 1 h in a 1 M $MgCl_2$ solution initially at pH 7.0. EDTA extractions were performed by suspending solids for 1 h in a 0.05M EDTA solution. A total of 17.5 g of each sample was subjected to the $MgCl_2$ extraction; half of this total mass was removed following the $MgCl_2$ extraction and half was subjected to the EDTA extraction. Solid-to-liquid ratios of 1 g:8 mL were used for both extractions. The extractions were conducted at room temperature and samples were continuously mixed by end-over-end rotation during equilibration periods. Materials were rinsed twice with deionized water following each step of the extraction. Filtered (0.2 μm) supernatant samples were collected from each of the extraction and rinse solutions for chemical analysis.

Electron Probe Microanalysis (EPMA). EPMA was conducted on a JEOL model 733 Superprobe using both energy-dispersive and wavelength-dispersive spectrometers (EDS and WDS). Samples for EPMA were prepared as epoxy suspensions on glass slides, polished smooth, and graphite coated. Samples were scanned manually at magnifications of 100× using backscattered electron (BSE) imaging to identify Pb-rich phases. Particles 1 μm or larger containing greater than 10% Pb were readily identified by this method. Ad-

ditional analyses of grain boundaries and particles of intermediate BSE brightness [e.g., sulfides and Pb-bearing Fe/Mn (hydr)oxides] were conducted on selected grains. A representative set of Pb-bearing grains, as identified by EDS screening, was quantitatively analyzed for 13 elements (Si, Al, Fe, Mn, K, Ca, Ti, Na, Mg, S, As, Pb, and Zn) using WDS. BSE images were collected at fixed brightness and contrast settings to enable automated estimation of volume percentages using standard image processing software (NIH Image).

X-ray Absorption Fine Structure (XAFS) Spectroscopy. Pb L_{III}-EXAFS data were collected at the Stanford Synchrotron Radiation Laboratory (SSRL) on wiggler beamlines 4-2 and 4-3 using Si(220) or Si(111) monochromator crystals. Six to twenty-five scans were collected and averaged for each sample in order to provide a usable EXAFS signal to at least k of 9 $Å^{-1}$ (13 380 eV). Data were collected in fluorescence mode using either an Ar-filled Stern-Heald ion chamber (*33*) or a 13 element solid-state Ge detector with filters selected to reduce scattered radiation (As or Se) and background fluorescence (Al). Data collection was conducted at ambient temperature and pressure and without sample desiccation. Energy was calibrated to the first inflection of a Pb-metal foil standard (13 055 eV) whose spectrum was collected simultaneously with the spectrum of each sample. EXAFS spectra were extracted from averaged data files by preedge subtraction followed by spline fitting using EXAFSPAK software (*34*). E_o for EXAFS was set to 13 070 eV. Raw data were truncated at 13 400 eV to avoid interference from the Bi L_{III} absorption edge (13 419 eV), arising due to Bi in the samples (up to 31 ppm).

Conventional shell-by-shell fitting was conducted using the OPT module of EXAFSPAK (*34*). Individual frequencies in the composite EXAFS (isolated by backtransforming a windowed region of the raw data Fourier transform) were fit using phase and amplitude functions generated by FEFF (*35*). Variables in these fits include the energy shift (ΔE_o), coordination number (N), radial distance (R), a Debye−Waller-type disorder factor (σ^2) for each shell, and a scale factor (S_o^2) applied to all shells in a fit. N and R values were derived by nonlinear least-squares fitting with σ^2 and S_o^2 fixed to 0.01 and 0.8, respectively, and E_o fixed to the best fit for the first shell. Previous model system studies indicate that R values derived in this manner are accurate to approximately ±0.02 Å for first shell distances (for discussion, see ref *36*) and somewhat larger for more distant shells [e.g., ±0.04 Å for second neighbors (*37*)]. N values extracted from this type of EXAFS fitting are generally accurate to ±1 (*36*). Fixing values of the amplitude reduction factors (S_o^2 and σ^2) facilitates comparisons of N values between fits.

Empirical EXAFS Fitting. Linear combinations of empirical model spectra were optimized, where the only adjustable fitting parameters were the fractions of each model compound spectrum contributing to the fit. Because EXAFS amplitudes are effectively normalized to a per-atom basis, the fraction of total Pb residing in a given component (mineral phase or other coordinatively distinct species) is given directly by the fraction of the corresponding model spectrum contributing to a fit. In other words, the fraction of a component in a fit of this type is equivalent to the atomic fraction of total Pb in that component. A useful corollary is that contributions from all components in a mixture should sum to unity. Best fits were derived by incrementally increasing the number of fit components and minimizing the fit residual. Fitting was conducted using k^3-weighted EXAFS spectra. Fits were optimized by minimizing the residual of the fit, defined as the normalized root square difference between the data and the fit. The range for the fit was varied as a function of data quality and in order to clarify/test contributions from minor components.

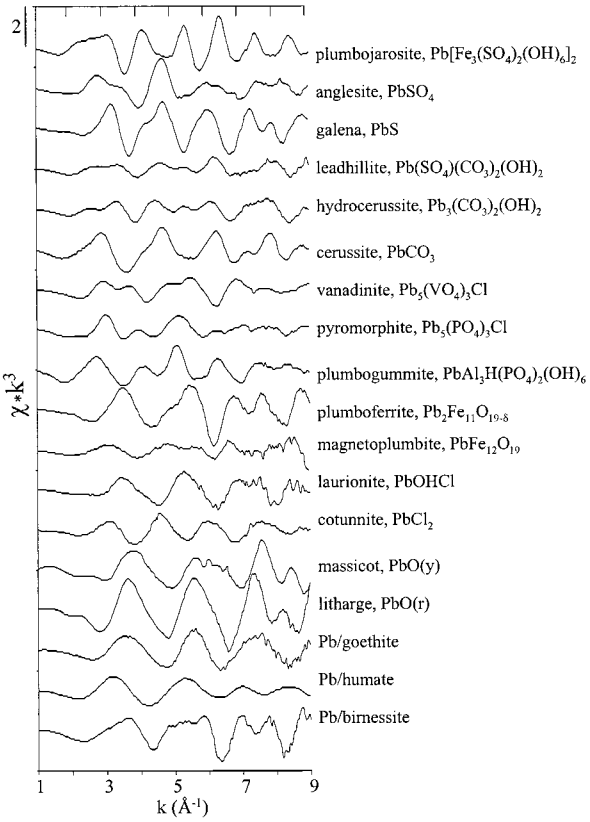

FIGURE 1. Selected Pb L_{III}-EXAFS spectra used as empirical models for linear least-squares fitting. Information regarding the sorption models is listed in Table 2. Additional models used for fitting include plattnerite (PbO_2), Pb adsorbed to hematite (Fe_2O_3) (see ref *38*), Pb−chloride ternary complex on goethite (see ref *59*), and aqueous species Pb^{2+} and $PbEDTA^{2-}$.

Model Set for EXAFS Fitting. A set of 22 Pb L_{III}-EXAFS reference spectra were collected for EXAFS fitting (Figure 1). This set of models was chosen based on the chemical associations of Pb noted by EPMA and the bulk mineralogy of the materials under study. Lead chloride and Pb-EDTA models were included to screen for possible reaction products after chemical extraction for those samples that were subjected to this procedure. Crystalline models were selected from the Stanford University Mineral Collection and confirmed by powder XRD. A tabular summary of first-shell Pb coordination for the Pb minerals used as EXAFS models, including additional discussion and references, is included as Supporting Information.

Sorption substrates [goethite (α-FeOOH), birnessite ("δ-MnO_2"), and humic acid] were selected specifically for their potential relevance to the Leadville site. Goethite and birnessite were selected because these and structurally similar minerals are common in natural weathering environments and because EPMA analyses of our samples showed strong associations between Pb and Fe and/or Mn (hydr)oxides. Humic acid was included as a general model for Pb associated with natural organic matter. Our use of Pb on goethite as a proxy for the general class of Pb adsorbed to Fe (hydr)-oxides is supported by previous EXAFS investigations that show similar structures for Pb on hematite (e.g., ref *38*) and HFO (e.g., ref *39*) and also by the fact that poorly crystalline hydrous iron oxides commonly have a goethite-like structure on the local (nm) scale (*40*). Furthermore, recently completed model system studies indicate that first- and second-shell distances observed for Pb sorption to goethite are essentially unchanged (ΔR < 0.03 Å) by the presence of carbonate and sulfate (*41*), which are expected

TABLE 2. Pb Coordination in Adsorption Complexes on Selected Surfaces as Determined by EXAFS Spectroscopy (Models Used for This Study in Italics)

				Pb−O				Pb-X			
surface	coverage (μmol/m^2)	N[a]	pH	R_{ave}	R_{min}	R_{max}	X	R_{ave}	R_{min}	R_{max}	refs[b]
goethite	2−4	3	5−7	2.27	2.26	2.28	Fe	3.34	3.31	3.36	*38*
hematite	2−10	6	6−8	2.28	2.27	2.29	Fe	3.29	3.27	3.31	*38*
muscovite		1		2.28							*52*
feldspar		1		2.28							*52*
humic acid		3	4−6	2.38	2.30	2.44	C	3.26	3.25	3.29	*45*
birnessite	1 wt %	1		2.30			Mn	3.79			*44*
goethite	*2*	*1*	*7*	*2.28*			*Fe*	*3.35*			
humic acid	*1 wt %*	*1*		*2.40*							see also ref *37*
birnessite	*0.4*	*1*	*6*	*2.32*			*Mn*	*3.76*			

[a] Number of samples. [b] Data collected at room temperature, except the humic acid spectrum (italics), which was collected at 15 K. [c] See also refs *25* and *39* for data collected at cryogenic temperatures and at higher coverages.

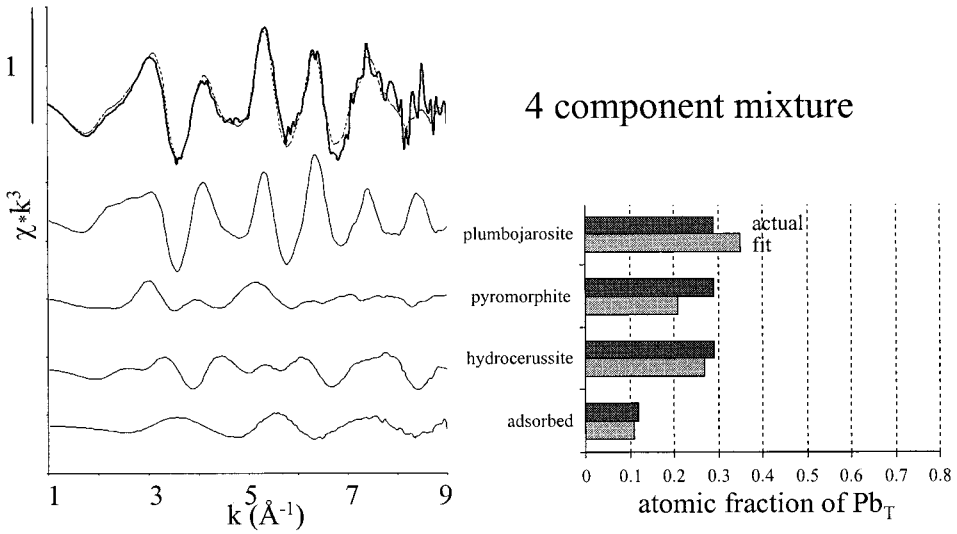

FIGURE 2. Pb L_{III}-EXAFS empirical fitting method test. Spectrum at top in bold is from a physical mixture of plumbojarosite, pyromorphite, hydrocerussite, and Pb(II) adsorbed to goethite (2 μmol/m^2, pH 7). Best fit is overlain as dashed line, and individual component spectra are shown scaled to their contributions to the fit.

to be two of the dominant inorganic ligands in the Leadville tailings selected for analysis.

Sorption models were prepared under controlled laboratory conditions. Pb on goethite and birnessite models were prepared in our laboratory and analyzed at room temperature as moist pastes. A synthetic model of Pb bound to humic acid was prepared and analyzed by Morin et al. as a part of a companion investigation of smelter-impacted soils from northern France (*37*); this sample was dried at room temperature and analyzed at 15 K. Note that EXAFS amplitudes in this last sample may be increased relative to comparable room temperature data, particularly at high *k*, due to decreased thermal vibrations at 15 K. In principle, this could cause underestimation of this component when fitting room temperature data. Goethite was prepared by Alexander Robinson (Department of Civil Engineering, Stanford University) according to the procedure described by VanGeen et al. (*42*) and was freeze-dried prior to use. Birnessite was synthesized according to procedures discussed by McKensie et al. (*43*) by Andrea Foster (Department of Geological and Environmental Sciences, Stanford University). Preparation conditions and quantitative EXAFS fitting results for the sorption samples used as empirical models are summarized in Table 2. The Pb sorbed on birnessite model was prepared under an actively purging humidified Ar atmosphere, and the Pb sorbed on goethite model was equilibrated with laboratory atmosphere (~350 ppm CO_2).

Quantitative shell-by-shell fitting confirms that Pb coordinations in our adsorption models are consistent with those reported in previous model system studies (see Table 2). Oxygen and Fe distances observed in the Pb sorbed on goethite model indicate that Pb forms dominantly bidentate edge-sharing complexes to $Fe(O,OH)_6$ octahedra as reported previously for Pb sorbed on goethite and hematite (*38*, *39*), and oxygen and Mn distances observed in the Pb sorbed on birnessite model are consistent with Pb adsorbing above and below vacancies in the MnO_2 layers of the birnessite structure (*44*). As noted previously (*25*), Pb sorbed to birnessite is readily distinguished from Pb sorbed to goethite and other Fe (hydr)-oxides. The spectrum used for Pb sorbed on humic acid is presented and discussed in a related paper (*37*) and is fit by a first shell Pb−O distance of 2.40 Å, consistent with previously reported values (*45*).

Results and Discussion

Empirical EXAFS Fitting Method Test. Three different mixtures of Pb compounds were prepared in known proportions and analyzed to test the accuracy of the linear least-squares fitting approach. The mixtures were composed of either two or four components with individual components accounting for 12−71% of Pb_T (e.g., Figure 2). Fitting results for the known mixtures deviate from actual atomic fractions by between −0.13 and 0.06 of Pb_T (3−28% of the actual fraction present), with an average deviation magnitude of 0.05 (12.6%). While contributions as low as 12% of Pb_T were

readily and accurately identified, our results suggest that contributions derived by this method should, in general, be considered accurate to ±25% of their stated value and that contributions less than 10% should be viewed with caution. Similar results have been reported using this method to fit *k*-weighted EXAFS data (*25*); fitting k^3-weighted spectra increases the sensitivity of the technique in general and particularly to higher *k* features.

Hamms Tailings. Pb-bearing phases detectable by EPMA include galena, phosphates, vanadates, and carbonates, as well as Fe-rich hydrous oxides and sulfates. Galena occurs both as isolated grains and associated with other sulfides, but was not detected in the fine fractions used for EXAFS analyses. Pb phosphates occur as isolated grains with Ca/Pb molar ratios ranging 0−0.5. Pb-vanadates and Pb-bearing Fe-rich (hydroxy)sulfates were detected only rarely in our sample of the Hamms tailings.

Volume estimates based on BSE imaging indicate that phases containing greater than ~10 wt % Pb (galena, lead phosphates, and lead carbonates) account for less than 50% of Pb_T in these materials, the balance occurring as phases with lower Pb concentrations and/or with particle sizes less than about 1 μm. EPMA data indicate that most of the balance occurs in association with fine grained Fe- and/or Mn-rich (hydr)oxides; analysis of these materials is hindered by their fine grain size, but they are typically dominated by iron (>50 wt % as Fe_2O_3) and contain less than 6% PbO, with varying amounts of Mn, Si, Al, and Zn. Species of this description have been widely identified in materials from the Leadville area (e.g., refs *1* and *3*) and are the most readily bioavailable class of Pb species of those tested by in vivo analysis (*4*).

Despite their significance, both in terms of total mass and bioavailability, the nature of the association between Pb and these Fe- and/or Mn-rich materials has not been definitively characterized in previous studies at Leadville. In general, these materials could contain Pb as microcrystalline (co)precipitates and/or as adsorption complexes. Model system investigations suggest that Pb(II) associated with Fe and Mn (hydr)oxides is likely bound as adsorption complexes (e.g., refs *20*, *38*, and *39*), although a number of studies have identified Pb/Fe/Mn "coprecipitates" as important sinks for Pb in natural systems (e.g., refs *46* and *47*) and direct structural characterization of naturally occurring "Pb/Fe/Mn-bearing" materials is generally lacking. Chemical extractions suggest that Pb is present in the Hamms materials as chemically bound surface complexes and/or EDTA-soluble (co)precipitates (see below).

Two fine-grained separates of the Hamms tailings (<100 and <10 μm) were analyzed by EXAFS spectroscopy. Empirical fitting shows that Pb speciation in these samples is dominated by Pb adsorbed to oxyhydroxide surfaces with additional contributions from the Pb-bearing apatite pyromorphite and hydrocerussite (Figure 3). These fits are consistent with EPMA results and confirm that Pb detected in Ca-bearing phosphates occurs in the apatite structure type. Furthermore, because Pb L_{III}-EXAFS spectra of Pb/Ca apatite solid solution members deviate substantially from the pure Pb endmember (pyromorphite) (*48*), our data indicate that Pb occurs either as discrete pyromorphite grains and/or as Pb-rich domains within a generally Pb-poor apatite phase. This finding is consistent with previous EXAFS results (*24*), which identified relatively pure pyromorphite occurring in association with Ca-rich phosphates in Derbyshire, England. The combination of adsorbed Pb (Pb on goethite) and pyromorphite is the best two-component fit of both the <10 μm and the <100 μm samples. The presence of both lead phosphates and adsorbed species in these materials shows that, while lead phosphates may effectively sequester Pb (e.g., ref *49*) and effectively compete with surface complexes for Pb (*50*), these processes are phosphate-limited in the Hamms tailings. The contribution of hydrocerussite to these fits, while relatively small, is supported by microprobe data and is consistent with the abundance of carbonate minerals in these tailings.

The identification of adsorbed Pb in these materials is important not only because it accounts for a large fraction of total Pb, but also because this type of species is the least accessible to identification and characterization by more conventional analytical techniques. Results from shell-by-shell fitting help clarify and confirm the results of our empirical fitting. In particular, the best two-shell fit to the <10 μm fraction (1.6 O at 2.28 Å and 0.3 Fe at 3.32 Å) corresponds directly with the two-shell fit to our Pb on goethite model (Table 2). It is important to note, however, that the presence of additional components beyond adsorbed Pb in the Hamms sample are indicated by the poor quality and low coordination numbers of the two-shell fit to this sample relative to the Pb on goethite model spectrum.

In short, shell-by-shell fitting illustrates that adsorbed Pb(II) is the primary component in the empirical fits because it accounts for the first-shell distance that dominates Hamms EXAFS spectra. The question thus becomes whether and to what extent this first-shell contribution is truly diagnostic of adsorbed Pb(II). A review of the mineralogical and EXAFS literature shows only a limited number of Pb(II) species with Pb−O distances as short as that observed in the Hamms tailings samples; these include Pb adsorbed to mineral substrate(s), Pb bound to organic molecules, and only a few inorganic crystalline compounds (see Supporting Information and ref *51*). Crystalline phases with comparably short Pb−O distances cannot, however, account for the observed Pb−O distance, since their EXAFS spectra invariably contain substantial second-shell contributions (and/or additional contributions from longer first-shell distances) which make them readily distinguishable from adsorbed Pb(II) (see Figure 1). Pb(II) bound to organic matter can also be ruled out as a significant Pb sink in these materials because the first-shell distances reported for such complexes are generally longer than the distance observed in the Hamms sample (Table 2; see also refs *25* and *45*) and because the tailings have a notably low organic carbon content (<0.01 wt. %). These additional considerations explain the results of our empirical fitting procedure and support our conclusion that ~40−50% of Pb_T in the Hamms tailings is adsorbed to mineral surfaces.

The adsorbed component of the EXAFS is, in particular, attributed to inner-sphere Pb(II) complexes on Fe-(hydr)oxide(s) based on the EXAFS data and the mineralogy and chemistry of the sample. Although Pb(II) adsorbed to aluminosilicate surfaces forms complexes with similarly short Pb−O distances (Table 2 (*52*)), EPMA data clearly indicate that the most common associations of Pb are with Fe and/or Mn (hydr)oxides. Given the known affinity of these (hydr)oxides for Pb under the near-neutral pH conditions of this tailings pile (e.g., refs *53* and *54*), we would expect Pb to be adsorbed to both of these classes of mineral surfaces. The greater contribution of Pb adsorbed to Fe (hydr)oxides to the EXAFS fit is consistent with the greater modal abundance of Fe (hydr)oxides than their Mn counterparts. While EPMA data clearly show Pb associated with Mn-rich (hydr)oxides, EXAFS data indicate that these account for a relatively small fraction of total Pb in this sample.

Apache Tailings. The same suite of Pb-bearing phases was detected by EPMA in the Apache materials as in the Hamms, but the relative abundances of these phases vary dramatically between the two piles. In contrast to the Hamms, Pb-bearing (hydroxy)carbonates in the Apache tailings are comparatively rare (the only Pb-bearing carbonates detected were found along the grain boundary of an anomalous dolomite grain), whereas lead vanadates and Pb-bearing Fe-rich (hydroxy)sulfates are more abundant. As in the Hamms,

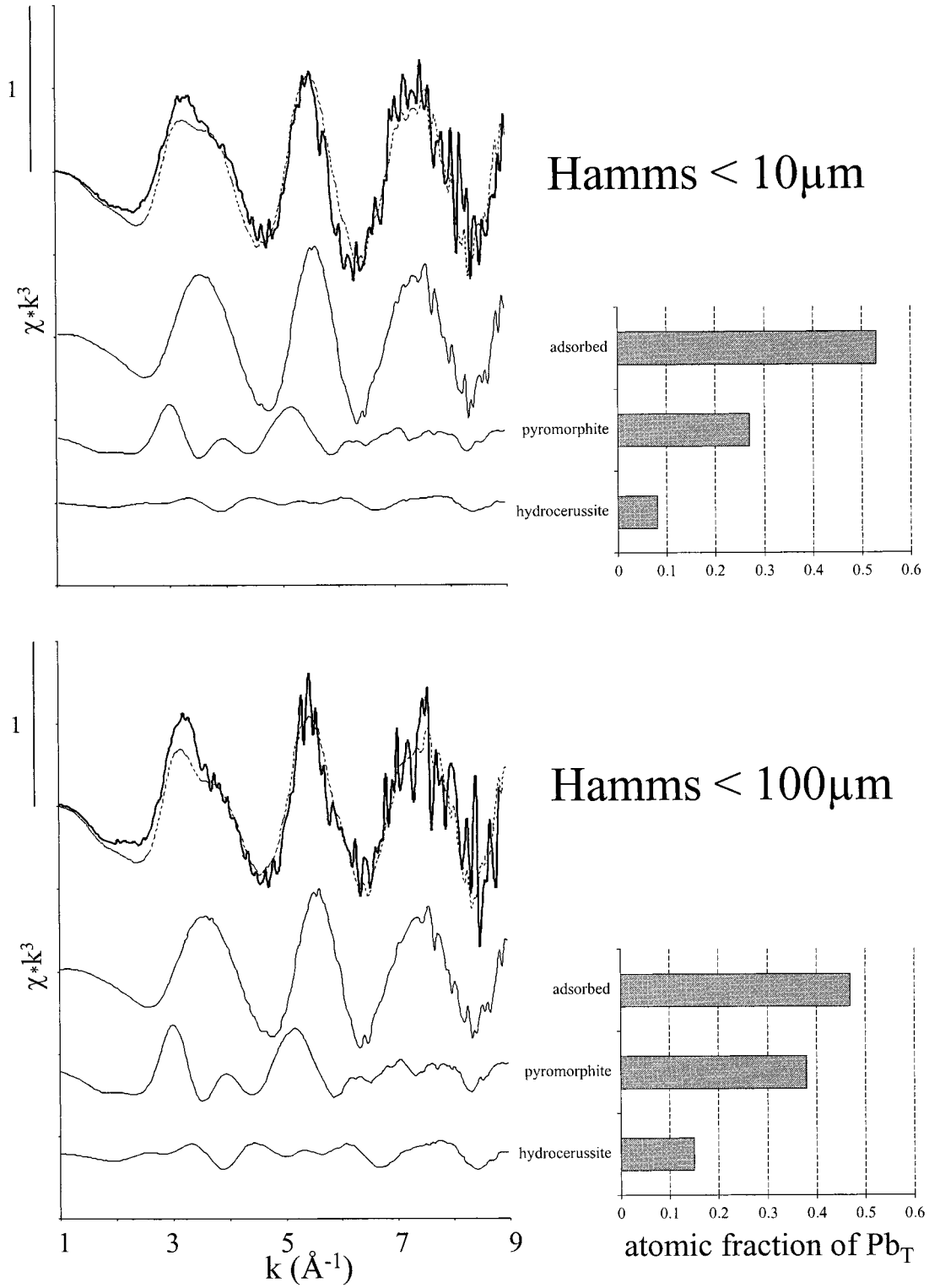

FIGURE 3. Pb L_{III}-EXAFS spectra of Hamms tailings fine fractions. Best fit linear combinations of model spectra are overlain as dashed lines. Component contributions are shown scaled to their contribution to the fit. The adsorbed Pb model is Pb on goethite (2 μmol/m^2, pH 7).

galena was not detected in the fine fractions used for EXAFS analyses, and phases containing greater than ~10 wt % Pb (galena, lead phosphates, and lead vanadates) and grain sizes greater than about 1 μm account for less than ~50% of total Pb based on BSE imaging.

Two fine-grained separates of the Apache tailings (<100 and <5 μm) were analyzed by EXAFS spectroscopy. Empirical fitting shows that the majority of Pb in both of these samples occurs in the jarosite structure (80−90% of total Pb in the <5 μm sample and about 50% in the <100 μm sample). Additional components included in the EXAFS fits are plumboferrite and vanadinite (Figure 4). Because the Pb L_{III}-EXAFS of plumbojarosite is dominated by backscattering from 6 Fe at 3.55 Å, and has only minor contributions from Pb backscatterers (nearest Pb neighbors are at 7.3 Å), the fit to our plumbojarosite model is interpreted as evidence for Pb-bearing jarosite and not necessarily for pure endmember plumbojarosite. The presence of Pb-bearing jarosite in these

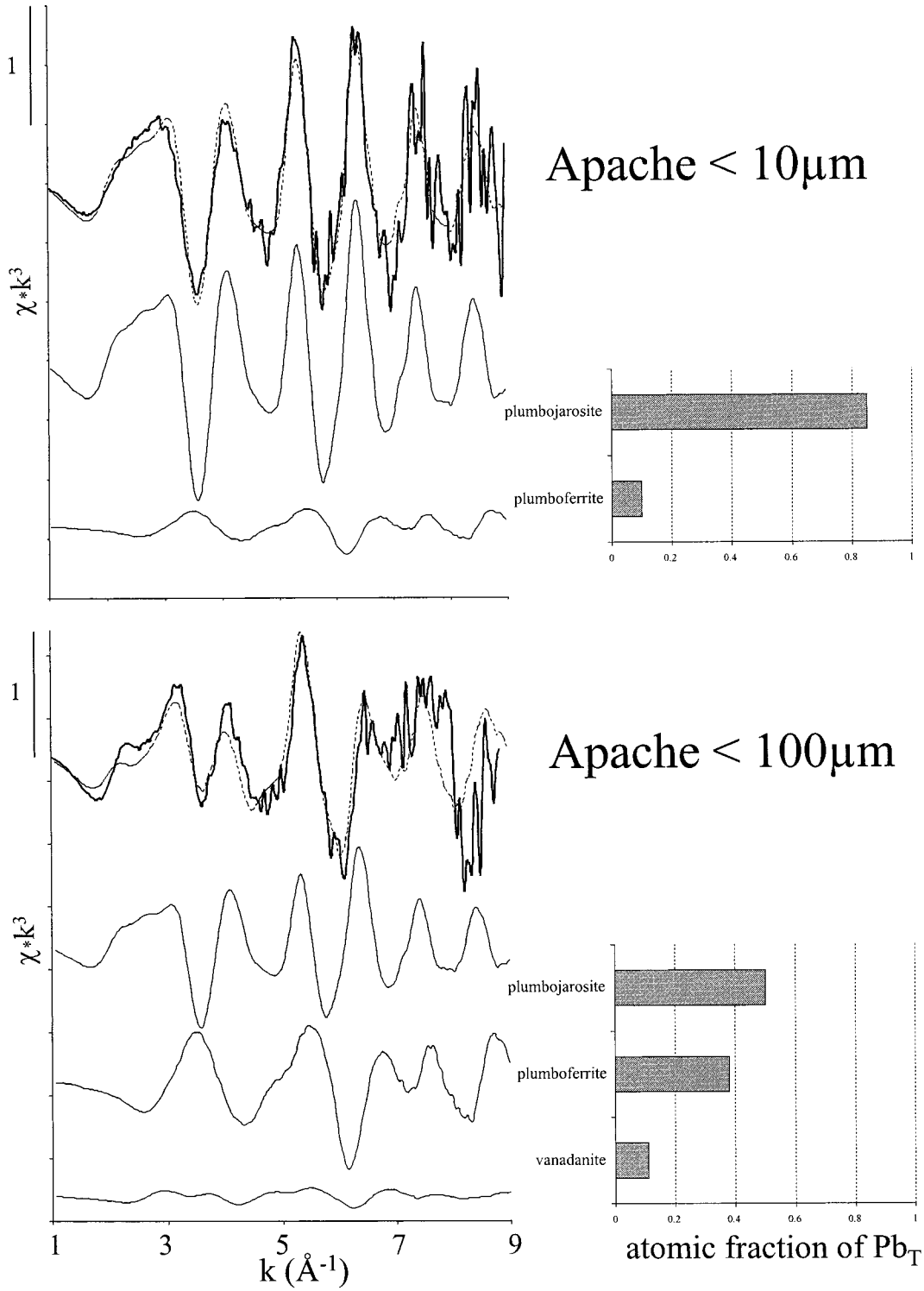

FIGURE 4. Pb L_{III}-EXAFS spectra of Apache tailings fine fractions. Best fit linear combinations of model spectra are overlain as dashed lines. Component contributions are shown scaled to their contribution to the fit.

samples is consistent with their low pH (for discussion, see refs *55*), detections of jarosite by XRD, and Pb-bearing Fe-rich sulfates by EPMA.

Contributions to these EXAFS spectra beyond Pb-bearing jarosites are less certain. In the <5 μm sample, additional component(s) are difficult to identify simply because, if present, they account for a relatively small fraction of total Pb. In contrast, the <100 μm spectrum clearly contains Pb-bearing phase(s) other than jarosites, since fitting this spectrum with plumbojarosite alone gives a poor fit and an unreasonably low total (0.4). The contribution of vanadinite to this spectrum (0.11), while too small to be definitive from EXAFS alone, is consistent with EPMA results. The more substantial contribution from a plumboferrite-like phase is also supported by microprobe results (strong Pb/Fe correlations) and gives the best possible two-component fit from our model set. Gross similarities between the plumboferrite and Pb sorbed on birnessite spectra, however, give rise to some ambiguity in this identification; in the spectrum of the <5μm fraction, either plumboferrite or Pb on birnessite gives a comparable two-component fit. Furthermore, since Pb uptake on birnessite occurs below pH 2 (*53*), Pb sorption to

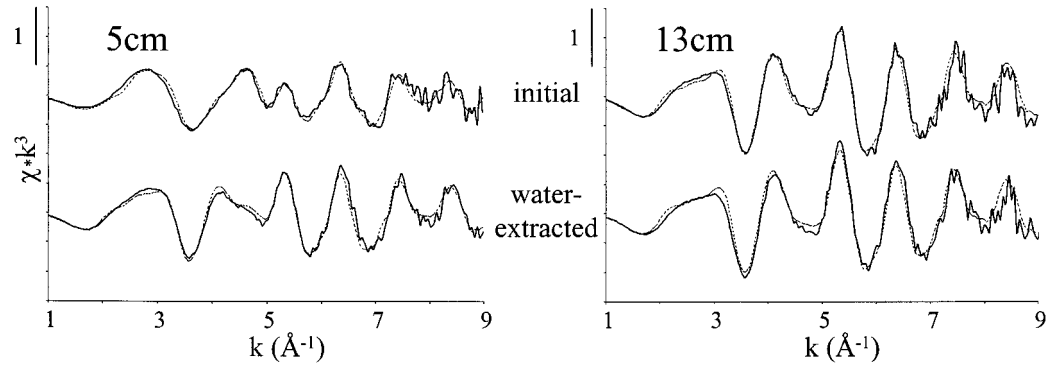

FIGURE 5. Pb L_{III}-EXAFS spectra of Arkansas River tailings fine fractions (<250 μm) collected ~13 km downstream from Leadville. Spectra are for 5 cm (left) and 13 cm (right) below ground surface in a single continuous core before and after water extraction (Smith et al., core no. 10 (*15*)). Best fit linear combinations of model spectra are overlain as dashed lines. The 5 cm samples are fit by a combination of anglesite (42% before extraction, and 24% after) and plumbojarosite (36% before extraction, and 63% after). The 13 cm samples are fit by plumbojarosite (81% before and after extraction) with minor contributions from plumboferrite (9% before extraction, 6% after). See Figure 1 for component spectra.

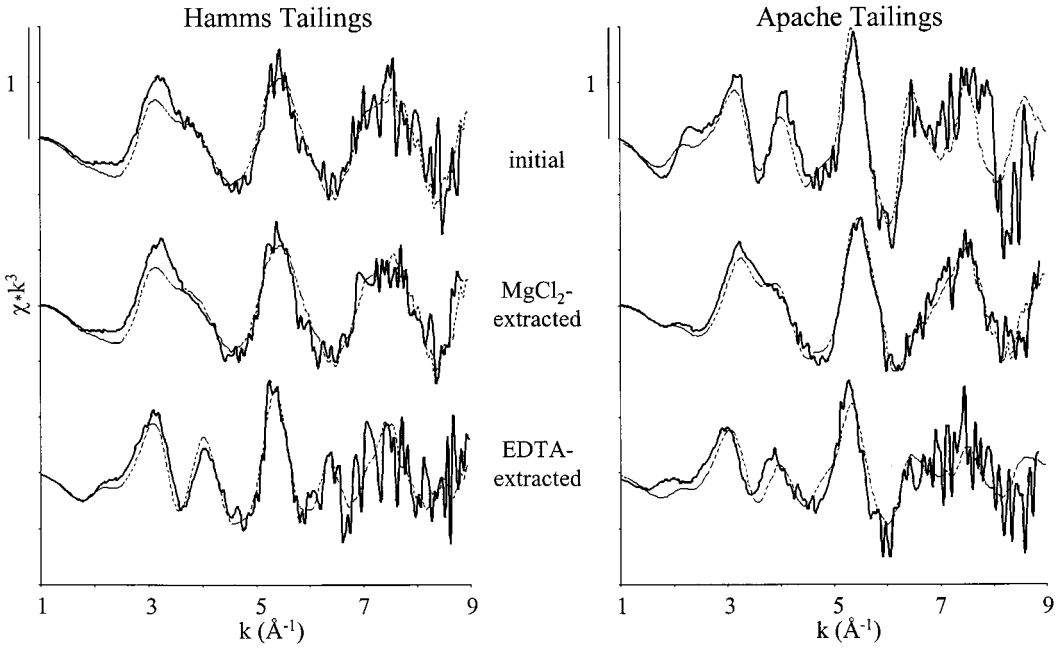

FIGURE 6. Pb L_{III}-EXAFS spectra of Hamms and Apache tailings fine fractions (<100 μm) before and after extraction by 1 M $MgCl_2$ (pH7) and 0.05 M EDTA. Best fit linear combinations of model spectra are overlain as dashed lines. Best fit to the Hamms tailings is unchanged after $MgCl_2$ extraction (47% Pb on goethite, 38% pyromorphite, and 15% hydrocerussite; see Figure 3). The post-EDTA Hamms spectrum is fit by 35% Pb(II) on goethite, 29% pyromorphite, and 34% plumbojarosite. The post-$MgCl_2$ spectrum of the Apache tailings materials is altered dramatically from the preextraction spectra, and is fit by 45% Pb on goethite, 20% plumbojarosite, 19% plumboferrite, 10% vanadinite, and 5% galena (cf. Figure 4). The post-EDTA Apache spectrum is fit by 25% plumbojarosite, 16% plumboferrite, 13% vanadinite, and 24% pyromorphite. See Figure 1 for component spectra.

Mn (hydr)oxides is geochemically reasonable even in these low pH tailings. In the larger size fraction, however, the plumboferrite model clearly provides a better fit than Pb/birnessite. Although plumboferrite is described as forming during maximum pressure and temperature conditions at the type locality in Jakobsberg, Sweden (*56*), materials of plumboferrite composition have been identified by EPMA and described as "mature phases" in mining-impacted weathering environments (*5*, *57*). Lacking thermodynamic data for this phase, it is not possible to evaluate whether plumboferrite could form as a secondary phase in the Apache tailings pile, but our results indicate that Pb does occur in a plumboferrite-like coordination in these tailings.

Arkansas River Tailings. Two samples of Arkansas River tailings were collected at depths of 5 and 13 cm below ground surface in a single continuous core. As noted in the Experimental Section, a previous investigation (*15*) found dramatic differences in both the bulk mineralogy (specifically the pyrite and jarosite percentages) and the water extractable Pb between these two samples. In particular, the 13 cm sample has a higher percentage of jarosite (17%) and lower percentage of pyrite (5%) than the 5 cm sample (7% jarosite and 70% pyrite), and the 5 cm sample has much higher water-extractable Pb than the 13 cm sample (*15*).

EXAFS analyses of the samples prior to water extraction show that the 13 cm sample (high jarosite, low water-extractable Pb) is dominated by Pb-bearing jarosite (81%) and that the 5 cm sample (high pyrite, high water-extractable Pb) consists of a mixture of Pb-bearing jarosite and anglesite (36 and 42%, respectively; Figure 5). These results suggest that anglesite dissolution may account for the greater water-extractable Pb observed in the 5 cm sample. Analyses following water extraction support this hypothesis, showing a dramatic decrease in the contribution of anglesite to the

5 cm sample (42% before extraction to 24% after) and essentially no change in the speciation of the 13 cm sample (Figure 5). Furthermore, since the water extraction removes less than 5% of Pb_T from the 5 cm sample, the relatively dramatic changes in Pb speciation with water extraction noted by EXAFS suggest that dissolution of anglesite is accompanied by precipitation of additional plumbojarosite. Taken together, these results clearly illustrate that formation of plumbojarosite controls the longer term fate of Pb in this low pH fluvial tailings environment.

Chemical Extractions of Hamms and Apache Samples. There was no detectable Pb removed by the $MgCl_2$ extraction (<0.1%), whereas the EDTA extraction removed 33 and 47% of total Pb (Pb_T) from the Apache and Hamms materials, respectively. As discussed in the Experimental Section, if the extractions functioned as intended, these results would indicate that <0.1% of Pb_T is present as readily soluble and/or weakly bound surface Pb species, while 33 and 47% of Pb_T is present as strongly bound inner-sphere type surface Pb complexes and/or EDTA-soluble phases [e.g., carbonates and/or poorly crystalline Fe (hydr)oxides] in the Apache and Hamms samples, respectively.

Direct analyses of these materials by EXAFS provide a more detailed, and in some important respects divergent, interpretation of the extraction results. Since no detectable Pb is removed from the solid phase in these samples by $MgCl_2$ extraction, the dramatic change in EXAFS spectra after this extraction in the Apache tailings sample is direct evidence for unintended redistribution of Pb species (Figure 6). More specifically, EXAFS fitting indicates that this redistribution is largely attributable to dissolution of Pb-bearing jarosites and subsequent readsorption of Pb released by this process onto Fe (hydr)oxides. Dissolution of jarosites during the $MgCl_2$ extraction is geochemically reasonable, given the low pH stability range for jarosite minerals (*55*), and is consistent with the observed drop in pH from 7 (initial pH of extraction solution) to 6 during this extraction.

EXAFS spectra of both the Apache and Hamms tailings materials provide evidence for removal of adsorbed Pb by EDTA (Figure 6). In the Apache materials, the removal of adsorbed Pb (present in this sample only after $MgCl_2$ "extraction") by EDTA is, to the sensitivity of our EXAFS fitting, completely effective. In the Hamms materials, EDTA removes ~75% of the Pb initially present as adsorbed species and also dissolves Pb-carbonates.

Environmental Implications. Pb speciation varies dramatically and systematically between different tailings materials from the Leadville area. While many of these species are readily identified by conventional EPMA, some of the most important in terms of transport and bioavailability are not [e.g., adsorbates and fine-grained (co)precipitates]. In this study, we have identified and characterized such species using EXAFS spectroscopy in combination with conventional analytical techniques. In the carbonate-rich, near-neutral pH Hamms tailings, Pb speciation is dominated by Pb(II) adsorbed to Fe (hydr)oxides; while such species have been suggested by a number of previous authors (e.g., refs *1*, *3*, and *58*), our analyses provide the first direct evidence for Pb adsorbates in materials from the Leadville area. In contrast, Pb-bearing jarosites account for the majority of Pb_T in both the low-pH Apache and Arkansas River tailings samples; while suggested by detections of jarosite by XRD and of Pb associated with Fe-rich sulfates by EPMA, EXAFS data provide the definitive evidence for Pb-bearing jarosites. These results do not necessarily suggest a direct connection between the Apache tailings and the Arkansas River tailings, but do suggest that Pb mobility and fate in both of these low pH environments are controlled largely by formation of Pb-bearing jarosites. The absence of adsorbed Pb in the low pH materials (Apache and Arkansas River tailings) and their presence in the near-neutral pH Hamms tailings are consistent with the well-known pH dependence of cation adsorption.

Acknowledgments

The authors owe thanks to John Bargar (SSRL) for assistance with data collection and for providing a number of model spectra, Andrea Foster (Stanford University) for assistance with data analysis and for providing birnessite, Sandy Robertson (Stanford University) for providing goethite, Guillaume Morin and Farid Juilliot (University of Paris) for providing the Pb on humate model spectrum, Kathy Smith (USGS) for providing samples of Arkansas River tailings, Stan Spencer and Kim Hedberg (Walsh and Associates Environmental Scientists and Engineers) for assistance in sample collection, and Margaret Staub (ASARCO) for permission to conduct the study on tailings samples from Leadville. We also thank the staff of SSRL for technical support. SSRL is supported by the United States DOE and NIH. Finally, we thank the DOE for supporting this research through Grant DE-FG03-93ER14347-A007 and the NSF for partial support through Grant EAR-9406490. In addition, the Kirby Summer Graduate Fellowship program in the School of Earth Sciences at Stanford and the Corning Foundation are thanked for fellowship support of J.D.O. during portions of this study.

Supporting Information Available

Figure of Leadville, CO, site map, and a table of first shell Pb coordination. This material is available free of charge via the Internet at http://pubs.acs.org.

Literature Cited

(1) Levy, D. B.; Barbarick, E. G.; Siemer; Sommers, L. E. *J. Environ. Qual.* **1992**, *21*, 185−195.
(2) Clements, W. H.; Kiffney, P. M. *Environ. Toxicol. Chem.* **1994**, *13*, 397−404.
(3) Kimball, B. A.; Callender, E.; Axtmann, E. V. *Appl. Geochem.* **1995**, *10*, 285−306.
(4) Casteel, S. W.; Brown, L. D.; Dunsmore, M. E.; Weis, C. P.; Henningsen, G. M.; Hoffman, E.; Brattin, W. J.; Hammon, T. L. *Bioavailability of lead in soil and mine waste from the California Gulch NPL Site Leadville, Colorado—DRAFT REPORT*, United States Environmental Protection Agency, 1997.
(5) Davis, A.; Drexler, J. W.; Ruby, M. V.; Nicholson, A. *Environ. Sci. Technol.* **1993**, *27*, 1415−1425.
(6) Link, T. E.; Ruby, M. V.; Davis, A.; Nicholson, A. D. *Environ. Sci. Technol.* **1994**, *28*, 985−988.
(7) Lion, L. W.; Altmann, R. S.; Leckie, J. O. *Environ. Sci. Technol.* **1982**, *16*, 660−666.
(8) Lind, C. J.; Anderson, L. D. *7th International Symposium on Water-Rock Interaction*; Rotterdam, Balkema, 1992; Vol. 1, p 397−402.
(9) Tessier, A.; Fortin, D.; Belize, N.; DeVitre, R. R.; Leppard, G. G. *Geochim. Cosmochim. Acta* **1996**, *60*, 387−404.
(10) Davis, A.; Ruby, M. V.; Goad, P.; Eberle, S.; Chryssoulis, S. *Environ. Sci. Technol.* **1997**, *31*, 37−44.
(11) Martin, C. J.; Al, T. A.; Cabri, L. J. *Environ. Geol.* **1997**, *32*, 107−113.
(12) Tingle, T. N. *Appl. Surf. Sci.* **1993**, *72*, 301−306.
(13) Walsh and Associates. *Lead Speciation Study, Leadville, CO*; ASARCO, Inc.: 1993.
(14) *California Gulch CERCLA Site−Metal Speciation Data Report−Leadville, CO*; United States Environmental Protection Agency: 1994.
(15) Smith, K. S.; Sutley, S. J.; Briggs, P. H.; Meier, A. L.; Walton-Day, K. *Tailings and Mine Waste '98 Conference*; Fort Collins, Colorado, 1998.
(16) Gruebel, K. A.; Davis, J. A.; Leckie, J. O. *Soil Sci. Soc. Am. J.* **1988**, *52*, 390−397.
(17) Xiao-Quan, S.; Bin, C. *Anal. Chem.* **1993**, *65*, 802−807.
(18) Coetzee, P. P.; Gouws, K.; Pluddemann, S.; Yacoby, M.; Howell, S.; den Drijver, L. *Water SA* **1995**, *21*, 51−60.
(19) Slavek, J.; Pickering, W. F. *Water Air Soil Pollut.* **1986**, *28*, 151−162.
(20) Ford, R. G.; Bertsch, P. M.; Farley, K. J. *Environ. Sci. Technol.* **1997**, *31*, 2028−2033.

(21) Teo, B. K. EXAFS: Basic principles of Data Analysis. *Inorganic Chemistry Concepts*; Berlin: Springer-Verlag, 1986; Vol. 9.
(22) Brown, G. E., Jr.; Calas, G.; Waychunas, G. A.; Petiau, J. X-ray absorption spectroscopy: Applications in Mineralogy and Geochemistry. In *Spectroscopic Methods in Mineralogy and Geology, Reviews in Mineralogy*; Hawthorne, F. C., Ed.; Mineralogical Society of America, 1988; Vol. 18, pp 431−512.
(23) Koningsberger, D. C.; Prins, R., Eds. *X-ray Absorption. Principles, Applications, Techniques of EXAFS, SEXAFS, and XANES*; John Wiley & Sons, New York, 1988.
(24) Cotter-Howells, J. D.; Champness, P. E.; Charnock, J. M.; Pattrick, R. A. D. *Eur. J. Soil Sci.* **1994**, *45*, 393−402.
(25) Manceau, A.; Boisset, M.-C.; Sarret, G.; Hazemann, J.-L.; Mench, M.; Cambier, P.; Prost, R. *Environ. Sci. Technol.* **1996**, *30*, 1540−1552.
(26) Hestberg, D.; Sayers, D. E.; Zhou, W.; Plummer, G. M.; Robarge, W. P. *Environ. Sci. Technol.* **1997**, *31*, 2840−2846.
(27) Szulczewski, M. D.; Helmke, P. A.; Bleam, W. F. *Environ. Sci. Technol.* **1997**, *31*, 2954−2959.
(28) Foster, A. L.; Brown, G. E., Jr.; Tingle, T. N.; Parks, G. A. *Am. Mineral.* **1998**, *83*, 553−568.
(29) O'Day, P. A.; Carroll, S. A.; Waychunas, G. A. *Environ. Sci. Technol.* **1998**, *32*, 943−955.
(30) Tessier, A.; Campbell, P. G. C.; Bisson, M. *Anal. Chem.* **1979**, *51*, 1, 844−851.
(31) Borggaard, O. K. *Clay Miner.* **1982**, *17*, 365−368.
(32) Rudd, T.; Lake, D. L.; Mehrotra, I.; Sterritt, R. M.; Kirk, P. W. W.; Campbell, J. A.; Lester, J. N. *Sci. Total Environ.* **1988**, *74*, 149−175.
(33) Lytle, F. *Nucl. Instrum. Methods Res.* **1984**, *226*, 542−548.
(34) George, G. N.; Pickering, I. F. *EXAFSPAK*; http://ssrl.slac.stanford.ed/~george/EXAFSPAK_FILES/EXAFS.HTML, access date 03/99; Stanford Synchrotron Radiation Laboratory, Stanford, CA, 1993.
(35) Zabinsky, S. I.; Rehr, J. J.; Ankudinov, A.; Albers, R. C.; Eller, M. J. *Phys. Rev. B* **1995**, *52*, 2295.
(36) O'Day, P. A.; Rehr, J. J.; Zabinsky, S. I.; Brown, G. E., Jr. *J. Am. Chem. Soc.* **1994**, *116*, 2938−2949.
(37) Morin, G.; Ostergren, J.; Juilliot, F.; Ildefonse, P.; Calas, G.; Brown, G. E., Jr. *Am. Mineral.* **1999**, *84*, 420−434.
(38) Bargar, J. R.; Brown, G. E., Jr.; Parks, G. A. *Geochim. Cosmochim. Acta* **1997**, *61*, 2639−2652.
(39) Manceau, A.; Charlet, L.; Boisset, M. C.; Didier, B.; Spadini, L. *Appl. Clay Sci.* **1992**, *7*, 201−223.
(40) Combes, J. M.; Manceau, A.; Calas, G.; Bottero, J. Y. *Geochim. Cosmochim. Acta* **1989**, *53*, 583−594.
(41) Ostergren, J. D.; Bargar, J. B.; Brown, G. E., Jr.; Parks, G. A. *J. Synch. Rad.* In press.
(42) Van Geen, A.; Robertson, A. P.; Leckie, J. O. *Geochim. Cosmochim. Acta* **1994**, *58*, 2073−2086.
(43) McKenzie, R. M. *Mineral. Mag.* **1971**, *38*, 493−502.
(44) Boisset, M. C. *Etude structurale des oxydes hydrates de fer et de manganese. Interaction avec une surface. Application au pigege du plomb dans le milieu naturel*, thesis; University of Paris 6 and 7, 1995.
(45) Xia, K.; Bleam, W.; Helmke, P. A. *Geochim. Cosmochim. Acta* **1997**, *61*, 2211−2221.
(46) Hem, J. D. *175th Meeting of the American Chemical Society*; American Chemical Society: Anaheim, CA, 1980; p 45−72.
(47) Erel, Y.; Morgan, J. J. *Geochim. Cosmochim. Acta* **1992**, *56*, 4157−4167.
(48) Laperche, V.; Traina, S. J. Immobilization of Pb by hydroxylapatite. In *Adsorption of Metals by Geomedia, Variables, Mechanisms, and Model Applications*; Jenne, E. A., Ed.; Academic Press: New York, 1998; pp 255−276.
(49) Laperche, V.; Traina, S. J.; Logan, T. J. *Environ. Sci. Technol.* **1996**, *30*, 3321−3326.
(50) Zhang, P.; Ryan, J. A.; Bryndzia, L. T. *Environ. Sci. Technol.* **1997**, *31*, 2673−2678.
(51) Bargar, J. R.; Brown, G. E., Jr.; Parks, G. A. *Geochim. Cosmochim. Acta* **1997**, *61*, 2617−2637.
(52) Farquhar, M. L.; Vaughan, D. J.; Hughes, C. R.; Charnock, J. M.; England, K. E. R. *Geochim. Cosmochim. Acta* **1997**, *61*, 3051−3064.
(53) Gadde, R. R.; Laitinen, H. A. *Anal. Chem.* **1974**, *46*, 2022−2026.
(54) Gunneriusson, L.; Lovgren, L.; Sjoberg, S. *Geochim. Cosmochim. Acta* **1994**, *58*, 4973−4984.
(55) Bigham, J. M.; Schwertmann, U.; Pfab, G. *Appl. Geochem.* **1996**, *11*, 845−849.
(56) Holstam, D.; Norrestam, R.; Sjodin, A. *Am. Mineral.* **1995**, *80*, 1065−1072.
(57) Davis, A.; Ruby, M. V.; Bergstrom, P. D. *Environ. Sci. Technol.* **1992**, *26*, 461−468.
(58) Smith, K. S.; Ficklin, W. H.; Plumlee, G. S.; Meier, A. L. *7th International Symposium on Water-Rock Interaction*; Balkema: Rotterdam, 1992; Vol. 1, pp 443−447.
(59) Bargar, J. R.; Brown, G. E., Jr.; Parks, G. A. *Geochim. Cosmochim. Acta* **1998**, *62*, 193−207.

Received for review July 1, 1998. Revised manuscript received February 16, 1999. Accepted February 23, 1999.

ES980660S